# COUPLING OF MAGNETIC ANALYSIS AND VIBRATIONAL MODAL ANALYSIS USING LOCAL FORCES

**Koen Delaere, Ronnie Belmans and Kay Hameyer**
*Dept. Electrical Eng. (ESAT), Div. ELEN, Katholieke Universiteit Leuven,*
*Kardinaal Mercierlaan 94, B-3001 Leuven, Belgium*
*EMail: koen.delaere@esat.kuleuven.ac.be*

**Ward Heylen, Paul Sas**
*Dept. Mechanical Eng., Div. PMA, Katholieke Universiteit Leuven,*
*Celestijnenlaan 300B, B-3001 Leuven, Belgium*
*EMail: paul.sas@mech.kuleuven.ac.be*

## Abstract

A weak coupling between the magnetic and the mechanical finite element model is established based upon energy considerations. The coupling term results directly into a finite element expression for the nodal electromagnetic reluctance forces. This expression uses the partial derivative of the magnetic stiffness matrix with respect to displacement. This partial derivative is calculated explicitly for the linear and the non-linear case. The resulting force distributions are used as source terms for a subsequent vibration analysis. The relative contribution of the stator's modal shapes to the deformation excited by these force distributions is calculated for all rotor positions. This allows us to solve the equation of motion for a selected set of modes and to predict the machine's noise and vibration spectrum at the design stage. As an example, the coupling is used to analyse the vibrational behaviour of a 6/4 switched reluctance machine.

## 1 Introduction

The electric machine's behaviour in generating vibrations and noise is determined by the electromagnetic field in the airgap and the mechanical structure of the machine. The link between the magnetic and the mechanical analysis is the electromagnetic force exerted by the magnetic field on stator and rotor. To predict stator deformations caused by a sequence of magnetic field distributions occurring during operation, a *local force* formulation is needed. Here, a finite element based expression for local electromagnetic reluctance forces is presented. These force distributions can be used as an input to a subsequent mechanical analysis, static (elasticity analysis) or time-harmonic (vibration analysis). For the modal shapes of the stator and the force distributions occurring during operation, *mode participation factors* (MPF) are determined as a function of rotor position. The MPF indicate the relative importance of a particular mode shape towards the machine's vibrations and noise. This way, the noise and vibration spectrum can be anticipated at the design stage. This modal vibration analysis is illustrated using a 2D finite element model of a 6/4 switched reluctance machine (SRM). The method can be readily extended to 3D problems.

## 2 The Magneto-Mechanical System

The finite element methods (FEM) for magnetostatic analysis as well as the FEM for elasticity analysis are based upon the minimisation of an energy function. The *elastic energy* stored in a body with deformation $a$ ($x_i=x_{i,0}+u_i$, $y_i=y_{i,0}+v_i$ , $a_i=[u_i\ v_i]^T$) is [1]

$$U = \frac{1}{2} a^T K a \,, \tag{1}$$

where $K$ is the mechanical stiffness matrix, determined by the structure's geometry and material properties $\rho$, $E$ and $\nu$, i.e. density, Young modulus and Poisson modulus. The column vector $a$ contains the unknown nodal displacements. For normal stator deformations, the mechanical system remains in the linear range ($\sigma \ll \sigma_{0.2}$). The *magnetic energy* stored in an (unsaturated) system with magnetic vector potential $A$ is [2]

$$W = \frac{1}{2} A^T M A \,, \tag{2}$$

where $M$ is the global magnetic 'stiffness' matrix, determined by the system's geometry and magnetic permeability $\mu$. The column vector $A$ contains the unknown nodal magnetic vector potentials. Considering the similar form of the energy expressions (1) and (2), it is investigated whether the following combined system of equations can support a coupled magneto-mechanical analysis:

$$\begin{bmatrix} M & D \\ C & K \end{bmatrix} \begin{bmatrix} A \\ a \end{bmatrix} = \begin{bmatrix} T \\ R \end{bmatrix}, \tag{3}$$

where $T$ is the magnetic source term vector representing the right hand side of the Poisson equation (source current density). $R$ is the mechanical source term vector representing forces other than those of electromagnetic origin (external forces). The coupling matrices $C$ and $D$ can be evaluated considering the total energy $E$ in the magneto-mechanical system (assuming the linear case):

$$E = U + W = \frac{1}{2} a^{\mathrm{T}} K a + \frac{1}{2} A^{\mathrm{T}} M A \,. \qquad (4)$$

The partial derivatives of $E$ with respect to the unknowns $[A \;\; a]^{\mathrm{T}}$ identify with the combined system (3):

$$\frac{\partial E}{\partial A} = MA + \frac{1}{2} a^{\mathrm{T}} \frac{\partial K(A)}{\partial A} a = T \,, \qquad (5)$$

$$\frac{\partial E}{\partial a} = \frac{1}{2} A^{\mathrm{T}} \frac{\partial M(a)}{\partial a} A + Ka = R \,, \qquad (6)$$

where $T\partial A$ represents the magnetic energy increase $\partial W$ and $R\partial a$ the mechanical energy increase $\partial U$. The coupling terms are now recognised as

$$D = \frac{1}{2} a^{\mathrm{T}} \frac{\partial K(A)}{\partial A} \,, \qquad (7)$$

$$C = \frac{1}{2} A^{\mathrm{T}} \frac{\partial M(a)}{\partial a} \,. \qquad (8)$$

The coupling term $D$ represents the dependency of mechanical parameters in $K$ on the magnetic field $A$, e.g. magnetostriction effects. The coupling term $C$ represents the dependency of magnetic parameters in $M$ on the mechanical displacement $a$. These coupling terms play an important role in the determination of forces related to both effects.

# 3 Electromagnetic Forces

Using the coupling terms $C$ and $D$, it is possible to solve the matrix system (3) directly. Solving this strongly coupled system requires an iterative solver that can handle a non-sparse asymmetrical system, e.g. a GMRES solver. Since convergence and computing speed can be expected to be poor for this total matrix, it is useful to examine the numerically weak coupled version of (3). In this and the next paragraph, it is assumed that the mechanical material properties $E$, $\nu$ and $\rho$ do not depend on vector potential $A$ (neglecting magnetostriction), so that the coupling term $D$ vanishes. Decoupling (3) leads to an explicit expression for the electromagnetic reluctance forces.

First we consider the *linear case*. When the mechanical equation (6) is rearranged into

$$Ka = R - \frac{1}{2} A^{\mathrm{T}} \frac{\partial M(a)}{\partial a} A = R - CA \,, \qquad (9)$$

the right hand side reveals an extra force $-CA$ acting on the mechanical subsystem $K$. Since all external forces are gathered in $R$, (9) reveals a means to calculate the internal reluctance forces, indicated by $F_{rel}$. The forces $F_{rel}$ are calculated from the previously computed vector potential $A_0$ and the partial derivative of the magnetic stiffness matrix $M$ with respect to deformation $a$:

$$F_{rel} = -\frac{1}{2} A_0^{\mathrm{T}} \frac{\partial M(a)}{\partial a} A_0 \,. \qquad (10)$$

The coupling term $C$ need not be calculated explicitly to find $F_{rel}$. This expression for $F_{rel}$ is also found directly by deriving magnetic energy $W$ (2) with respect to displacement $a$ [3]:

$$F_{rel} = -\frac{\partial W}{\partial a} = -\frac{\partial}{\partial a}\left[\frac{1}{2} A^{\mathrm{T}} M(a) A\right], \qquad (11)$$

where the unknowns $A$ have to be considered constant (constant flux), so that again $A$=$A_0$.

In the *non-linear case* (and neglecting magnetostriction, $D$=0), the magnetic stiffness matrix $M$ becomes a function of both vector potential and deformation, so that (5) reduces to

$$T = M(A,a)\, A \,. \qquad (12)$$

The magnetic energy $W$ is now given by the integral

$$W = \int_0^A T^{\mathrm{T}} dA \,. \qquad (13)$$

The pair of variables ($A$,$T$) plays the same role towards energy and co-energy as the more common pair flux and current ($\psi$,$i$). Again, the force $F_{rel}$ is found as the change of magnetic energy $W$ with respect to deformation $a$ and keeping flux constant ($A$=$A_0$):

$$F_{rel} = -\frac{\partial W}{\partial a} = -\frac{\partial}{\partial a}\int_0^A T^{\mathrm{T}} dA \,,$$

$$= -\int_0^{A_0} A^{\mathrm{T}} \frac{\partial M(A,a)}{\partial a} dA \,, \qquad (14)$$

where $M^{\mathrm{T}}$=$M$ was used. When $M$ is a function of $a$ only, (14) reduces to the linear expression (10). Rather than calculating a finite energy difference between two finite element solutions, the partial derivatives in (10) and (14) represent more accurately the essence of virtual work [4]. There is no need for a second magnetic finite element solution and no numerical derivations are performed.

When the coupling term $C$ is replaced by the force $F_{rel}$, the system (3) is decoupled into

$$\begin{bmatrix} M & 0 \\ 0 & K \end{bmatrix} \begin{bmatrix} A \\ a \end{bmatrix} = \begin{bmatrix} T \\ R + F_{rel} \end{bmatrix}, \qquad (15)$$

which can be solved with a simple cascade procedure using solvers for positive-definite, symmetric matrices.

First the magnetic system $MA=T$ is solved, giving $A_0$. Then $F_{rel}$ is evaluated using (10) or (14) and becomes an extra force acting on the mechanical system $Ka = R + F_{rel}$. This scenario can be extended to the time-harmonic case to calculate mechanical vibrations, but this approach is limited to a single frequency. The method using Mode Participation Factors presented in sections 6.2 and 6.4 does not have this restriction. First, the force expression (14) will be derived analytically into a form that can be readily implemented into finite element code.

# 4 Finite Element Expression for $\partial M/\partial a$

The derivation $\partial M/\partial a$ is illustrated for the non-linear case, using first order 2D triangular elements for simplicity. For the magnetic element matrix [5]

$$M_{ij}^e = \frac{\nu}{4\Delta}[b_i b_j + c_i c_j]\,, \tag{16}$$

with reluctivity $\nu$, element area $\Delta$ and the familiar shape function coefficients $a_1=x_2y_3-x_3y_2$, $b_1=y_2-y_3$, $c_1=x_3-x_2$. The partial derivative of (16) with respect to $u_1$ ($a_i=[u_i\, v_i]^T$) is

$$\frac{\partial M_{ij}^e}{\partial u_1} = \frac{\nu}{4\Delta}\begin{bmatrix} 0 & c_1 & -c_1 \\ c_1 & 2c_2 & c_3-c_2 \\ -c_1 & c_3-c_2 & -2c_3 \end{bmatrix} - \frac{b_1}{2\Delta}M_{ij}^e + \frac{\partial\nu}{\partial u_1}\frac{M_{ij}^e}{\nu}\,. \tag{17}$$

Similar expressions are found for the partial derivative of $M^e$ with respect to alternative displacements ($u_2$, $u_3$, $v_1$, $v_2$ and $v_3$).
The third term in (17) requires some attention. The reluctivity $\nu$ depends on flux density $B$ according to the saturation characteristic of the material. In the finite element code used here, the material characteristic is stored in $\nu(B^2)$ format [2][5]. For first order triangles, $B^2$ is given by

$$B^2 = B_x^2 + B_y^2 = \frac{1}{4\Delta^2}\left(c_1A_1 + c_2A_2 + c_3A_3\right)^2 + \frac{1}{4\Delta^2}\left(b_1A_1 + b_2A_2 + b_3A_3\right)^2, \tag{18}$$

where $b_i$ and $c_i$ are the common shape function coefficients and $A_i$ is the vector potential on node $i$. Since in (18) only $c_2$, $c_3$ and $\Delta$ depend on $u_1$, the third term in (17) can be calculated explicitly:

$$\frac{\partial\nu}{\partial u_1} = \frac{d\nu(B^2)}{dB^2}\frac{\partial B^2}{\partial u_1} \tag{19a}$$

$$= \frac{d\nu(B^2)}{dB^2}\frac{1}{\Delta}\left[B_x\left(A_2 - A_3\right) - b_1B^2\right] \tag{19b}$$

$$= \frac{d\nu(B^2)}{dB^2}\frac{b_1}{\Delta}\frac{\sin\gamma\,\sin(\alpha-\gamma)}{\cos\alpha}\,B^2 \tag{19c}$$

$$= \frac{d\nu(B^2)}{dB^2}\,G_{u1}\,B^2\,. \tag{19d}$$

In (19c), $\alpha$ is the angle between the $y$-axis and the edge between nodes 2 and 3, and $\gamma$ is the angle between $\vec{B}$ and the $x$-axis. In (19d), all factors independent of $B^2$ are gathered in $G_{u1}$. The actual value of $d\nu/dB^2$ is retrieved from the material characteristic. The factor $d\nu/dB^2$ acquires significant values only in elements that are heavily saturated; in these elements the third term in (17) becomes an important force component and must not be neglected.
In the non-linear expression (14), the integral values of the three terms in (17) are required. The integrals are calculated per element ($A_0=[A_{1,0}\, A_{2,0}\, A_{3,0}]^T$) using $A=tA_0$, so that $dA=A_0dt$, $B^2= B_0^2\,t^2$ and $d(B^2)=2\,B_0^2\,tdt$. For the first two terms in (17), the integral counterpart is found by replacing $\nu$ by the following integral:

$$\nu \rightarrow \frac{1}{2B_0^2}\int_0^{B_0^2}\nu(B^2)\,d(B^2)\,, \tag{20}$$

where $B_0$ is the actual value of the flux density in the element under consideration. The integral of the third term in (17) reduces to

$$\int_0^{A_0} A^T\frac{\partial\nu}{\partial u_1}\frac{M_{ij}^e}{\nu}dA = \frac{1}{\nu}A_0^T M_{ij}^e A_0\left(\int_0^1\frac{\partial\nu}{\partial u_1}t\,dt\right), \tag{21}$$

since $M_{ij}^e/\nu$ is short for $[b_ib_j+c_ic_j]/4\Delta$ and does not depend on $\nu$ or $A$. Using (19d), the integral in (21) becomes

$$\int_0^1\frac{\partial\nu}{\partial u_1}t\,dt = G_{u1}\int_0^1\frac{d\nu}{dB^2}B^2\,t\,dt \tag{22}$$

$$= \frac{G_{u1}}{2B_0^2}\int_0^{B_0^2}\frac{d\nu}{dB^2}B^2\,d(B^2) \tag{23}$$

$$= \frac{G_{u1}}{2B_0^2}\int_{\nu^*}^{\nu_0}B^2 d\nu\,, \tag{24}$$

where $\nu^*$ is the reluctivity in the linear part of the material characteristic. From the integral in (24) it is seen that the third term in (17) is linked to the co-energy in the system, while the first two terms of (17) are linked to the energy integral in (20). The relation between both energies is given by

$$\int_{\nu^*}^{\nu_0}B^2\,d\nu = B_0^2\nu_0 - \int_0^{B_0^2}\nu(B^2)\,d(B^2)\,, \tag{25}$$

so that only one integral needs to be evaluated.
Similar expressions are found for the partial derivatives with respect to the other displacements ($u_2$, $u_3$, $v_1$, $v_2$ and $v_3$).

# 5 Magnetostriction

The coupling term $D$ is treated in a dual manner to evaluate forces related to magnetostriction. Rearranging (5) into

$$M\,A = T - \frac{1}{2} a^{\mathrm{T}} \frac{\partial K(A)}{\partial A} a = T - D\,a\,, \tag{26}$$

reveals an extra current density source–$Da$ acting on the magnetic subsystem $M$. This reveals a means to represent magnetostrictive effects by equivalent current densities, indicated with $J_m$. The current density sources $J_m$ are calculated from mechanical displacement $a$ and the partial derivative of the mechanical stiffness matrix $K$ with respect to magnetic vector potential $A$:

$$J_m = -Da = -\frac{1}{2} a^{\mathrm{T}} \frac{\partial K(A)}{\partial A} a\,. \tag{27}$$

The coupling term $D$ need not be calculated explicitly to find $J_m$. This expression for $J_m$ is also found directly by deriving elastic energy $U$ (1) with respect to magnetic vector potential $A$:

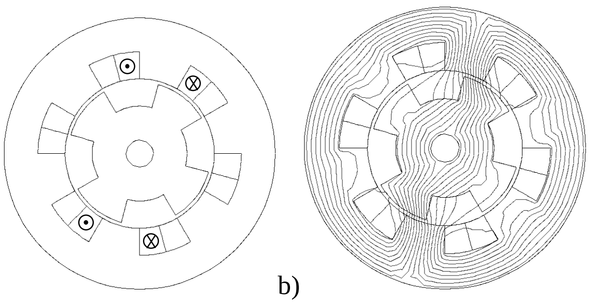

a) b)

Figure 1: a) Geometry of the 6/4 SRM and
b) magnetic flux lines for excitation according to a).

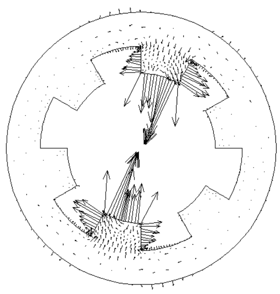

Figure 2: Force distribution calculated from the magnetic field in Fig.1b, using (14).

$$J_m = -\frac{\partial U}{\partial A} = -\frac{\partial}{\partial A}\left[\frac{1}{2} a^{\mathrm{T}} K(A)\, a\right], \tag{28}$$

where the unknowns $a$ have to be considered constant (virtual work principle).

# 6 Example: 6/4 SRM

## 6.1 Nodal Forces

The geometry of the example 6/4 SRM is shown in Fig.1a. For this rotor position, the coil system indicated is current excited and generates the magnetic field shown in Fig.1b. This magnetic field is used to evaluate the reluctance forces $F_{rel}$ acting on the stator structure. Fig.2 shows the force distribution calculated for the non-linear case, using (14). The radial forces acting on the teeth are larger than the tangential forces. The radial forces do not produce torque but do cause stator deformation.

## 6.2 Mode Shapes and Modal Participation

Using the stator's mechanical matrices $K$ (stiffness), $M_m$ (mass) and $C_m$ (damping), the eigenvectors and eigenvalues of the mechanical structure are found. These

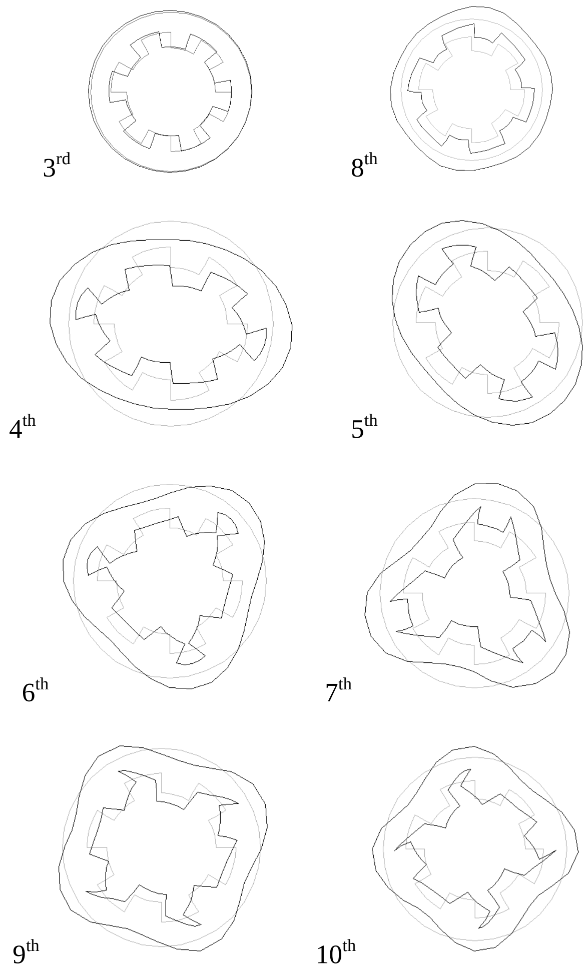


Figure 3: Selected modal shapes for the 6/4 SRM stator structure. The mode numbers are assigned according to ascending eigenfrequency.

constitute the stator deformation mode shapes. Several 2D mode shapes are shown in Fig.3; the machine mounting is not considered in determining the mode shapes. Accurate vibration analysis has to make use of 3D mode shapes [6]. The *mode participation factor* is defined as [7]:

$$\Gamma_i = \frac{\phi_i{}^T p}{\phi_i{}^T M_m \, \phi_i} , \tag{29}$$

where the vectors $\phi_i$ and $p$ are the $i^{\text{th}}$ mode shape and the force distribution respectively. The mode participation factor (MPF) indicates the correlation between force pattern $p$ and mode shape $\phi_i$ (Fig.4). To calculate (29), the mechanical mesh needs to be mapped onto the magnetic mesh [8].

Fig.5 shows the MPF as a function of rotor position (resolution: 1º) for ovalization modes 4 and 5, triangular modes 6 and 7, shrinking mode 8 and squaring modes 9 and 10. Since there is no triangular symmetry in the system, modes 6 and 7 are hardly excited compared to the other modes. Mode 8 represents the uniform shrinking and expanding of the stator frame; this mode is excited with the same sign (shrinking) for all rotor positions, with a relatively small ripple.

## 6.3 Torque

One could expect that the MPF of the 3rd mode shape, the rigid body rotation, is a measure for the instantaneous

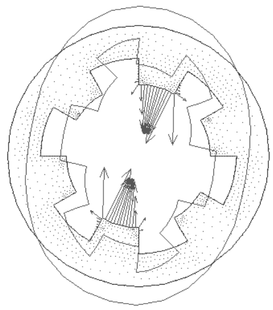

Figure 4: Illustration of Equation (29) correlating force pattern $p$ and mode shape $\phi_i$

torque of the SRM. However, the torque $T$ can be calculated more accurately using the cross-product

$$T = \sum_{i=1}^{N} \vec{F}_i \times \vec{r}_i \ , \tag{30}$$

where $\vec{F}_i$ is the $i^{\text{th}}$ nodal force vector with position $\vec{r}_i$ ($N$ = total number of nodal forces). Fig.6 compares the two methods for calculating the torque. It can be seen that the MPF for the rigid body rotation gives only a very coarse estimate of the torque.

## 6.4 Modal Analysis

The MPF $\Gamma_i$ have been determined as a function of rotor position. When a constant rotor velocity is assumed, in

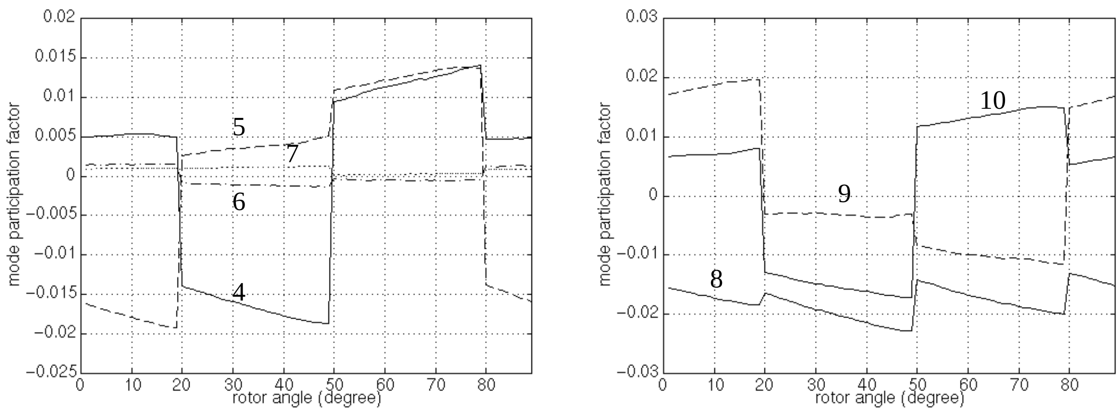


Figure 5: Mode participation factors as a function of rotor position.

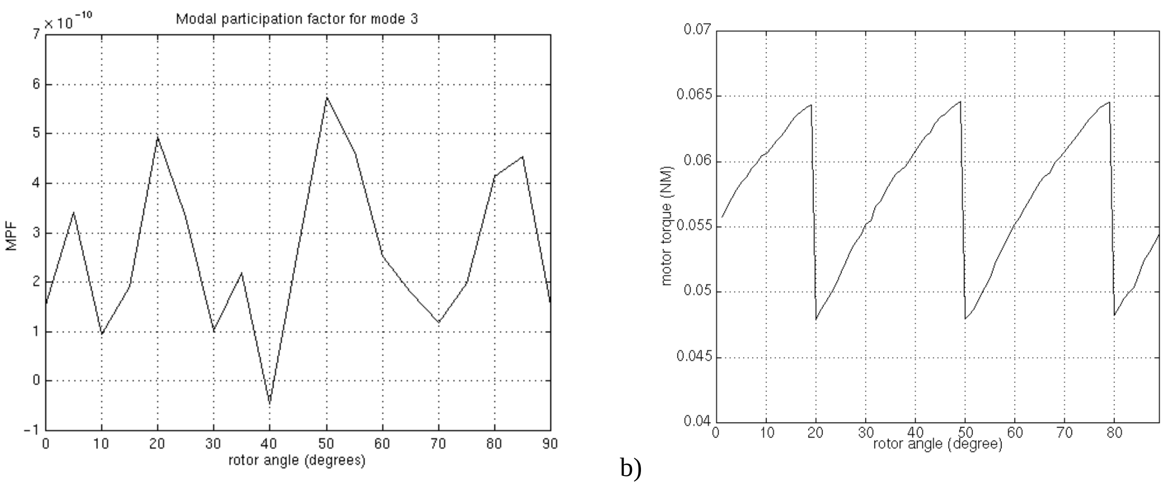


a) b)

Figure 6: a) Mode participation factor of the rigid body rotation (3rd mode),
b) Torque of the 6/4 SRM as a function of rotor position, calculated using (30).

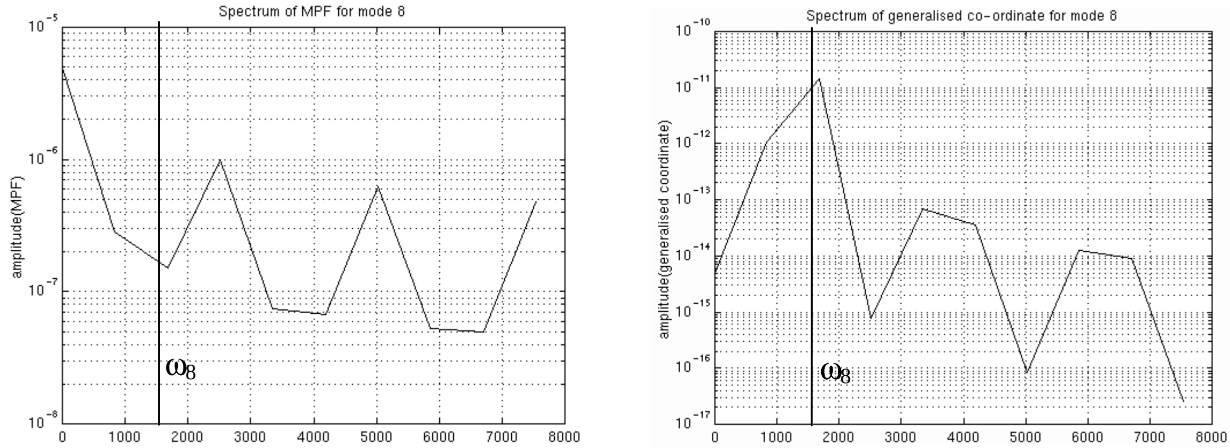


a) angular frequency (rad/s)
b) angular frequency (rad/s)

Figure 7: a) Spectrum of $\Gamma_8$ and b) generalised co-ordinate $Q_8$.

this case 2000 rpm, the MPF are also known as a function of time $\Gamma_i(t)$. Now the set of equations

$$\ddot{q}_i + 2\zeta_i \omega_i \dot{q}_i + \omega_i^2 q_i = \Gamma_i(t) \tag{31}$$

can be solved for a selected set of significant modes $\phi_i$. In (31), $q_i$ is the generalised (modal) co-ordinate of mode $i$, $\omega_i$ is the mode's circular eigenfrequency and $\zeta_i$ is the modal damping factor. Only when the mechanical damping is assumed to be proportional ($C_m=\alpha M_m+\beta K$), the system of equations (31) can be decoupled and solved separately [7]. In this analysis, damping is neglected ($\zeta_i$=0). The equations (31) are solved in the frequency domain after applying a discrete Fourier transformation:

$$Q_i(k\Delta\omega) = \frac{\Gamma_i(k\Delta\omega)}{-(k\Delta\omega)^2 + \omega_i^2}, \tag{32}$$

where $Q_i$ is the spectrum of $q_i(t)$ and $\Delta\omega=2\pi\Delta f$ with $\Delta f$=133Hz (rotor angle resolution is 1°).

Fig.7a shows, in semi-log scale, the discrete spectrum $\Gamma_8(k\Delta\omega)$ of the MPF of the 8$^{th}$ mode (uniform shrinking) with eigenfrequency $f_8$=262 Hz ($\omega_8$=1647 rad/s). Fig.7b shows the corresponding spectrum $Q_8(k\Delta\omega)$ of the generalised co-ordinate $q_8(t)$. Note how the DC-component of the MPF acting on the 8$^{th}$ mode is filtered out, while the excitation around 1647 rad/s (the 8$^{th}$ mode's eigenfrequency) is amplified. The modal spectra for all selected modes can be found in this way and summed to predict the motor's entire vibration spectrum.

# 7 Conclusions

A numerically weak coupling between magnetic and mechanical analysis is derived, leading to a finite element based expression for the nodal electromagnetic reluctance forces. This expression is based on the partial derivatives of the magnetic stiffness matrix and yields the distribution of local forces. The partial derivatives and their integrals (for saturated systems) are presented in a form that can be readily implemented in finite element code. The resulting force pattern can be used for elastic or vibrational analysis, torque calculation or any other post-processing action. The stator modal shapes and their participation factor in the force distribution are calculated for one rotor position and a single time instant. Repeating this analysis for all rotor positions allows us to solve the modal equations of motion in the frequency domain and anticipate the stator resonances and the noise frequency spectrum at the design level.

# 8 Acknowledgement

The authors are grateful to the Belgian "Fonds voor Wetenschappelijk Onderzoek Vlaanderen (FWOV)" for its financial support; Koen Delaere has a FWOV scholarship. The authors thank the Belgian Ministry of Scientific Research for granting the IUAP No.P4/20 on Coupled Problems in Electromagnetic Systems. The research Council of the K.U.Leuven supports the basic numerical research.

# 9 References

[1] O.C. Zienkiewicz, R.L. Taylor, *The Finite Element Method*, McGraw-Hill 1989.

[2] P.P. Silvester, R.L. Ferrari, *Finite Elements for Electrical Engineers, Second Edition*, Cambridge University Press, 1990.

[3] Z. Ren, “Comparison of different force calculation methods in 3D finite element modelling”, *IEEE Trans.Magn.*, vol 30, no.5, pp.3471-3474, 1994.

[4] J.L. Coulomb, G. Meunier, "Finite element implementation of virtual work principle for magnetic or electric force and torque computation", *IEEE Trans.Magn*. vol 20, no.5, pp.1894-1896, 1984.

[5] K.J. Binns, P.J. Lawrenson, C.W. Trowbridge, *The Analytical and Numerical Solution of Electric and Magnetic Fields*, John Wiley & Sons, 1992.

[6] D.Verdyck, *Mathematical modeling of invertor generated stator vibrations in electric machines*, Ph.D. Thesis (in Dutch), K.U.Leuven, Dec.1993.

[7] W.T. Thomson, *Theory of Vibrations with Applications, Fourth Edition*, Prentice-Hall 1993.

[8] R. Wait, A.R. Mitchell, *Finite Element Analysis and Applications*, John Wiley & Sons, 1985.